European Polymer Journal 48 (2012) 1485–1494

Contents lists available at SciVerse ScienceDirect

European Polymer Journal

journal homepage: www.elsevier.com/locate/europolj

Emission color tuning of copolymers containing polyfluorene, benzothiadiazole, porphyrin derivatives

Ho Jun Song, Doo Hun Kim, Tae Ho Lee, Doo Kyung Moon *

Department of Materials Chemistry and Engineering, Konkuk University, 1 Hwayang-dong, Gwangjin-gu, Seoul 143-701, Republic of Korea

ARTICLE INFO

Article history:
Received 8 April 2012
Received in revised form 31 May 2012
Accepted 6 June 2012
Available online 15 June 2012

Keywords:
Porphyrin
Fluorene
Conjugated polymer
WPLED

ABSTRACT

Copolymer containing benzothiadiazole (BT) and porphyrin (POR) derivatives as dopants (<0.3 mol%) was synthesized to polyfluorene (PF) backbone using Suzuki coupling reaction. The synthesized polymer was thermally stable and soluble in general organic solvents. UV–vis spectra of the polymer showed the similar behaviors in solution and on film. However, PL spectra was similar to PF in solution, but its peak increased around 520 and 612 nm as BT and POR, the dopants, went up in casting film. The more POR increased, the more effective Forster energy transfer was observed by POR than BT in PF. The device was made in ITO/PEDOT:PSS/polymer/BaF_2/Ba/Al structure. For PFB02P05 polymer, the luminous efficiency was 0.66 cd/A, the power efficiency 0.29 lm/W and the maximum brightness 936 cd/m^2. CIE coordinate (0.36, 0.34) was closer to pure white. For PFB15P20, the luminous efficiency was 1.40 cd/A, the power efficiency 0.32 lm/W, the maximum brightness 5997 cd/m^2. PFB15P20 demonstrated the best performance as green emission.

1. Introduction

For dozens of years, π-conjugated polymer have been applied to and examined in diverse kinds of application fields including organic light emitting diode (OLED) [1–4], organic photovoltaic cell (OPV) [5–9], and organic thin film transistor (OTFT) [10–13]. In particular, the polymer light emitting diode (PLED) has the advantage to be made in large scale using the screen printing as compared to the small molecule using vacuum coating. Thus, it has been drawing substantial attention as the next generation material in display field. Furthermore, it attracted substantial attention in flexible display field because of the flexibility of polymer film [8,14].

A number of researches has been focusing on PLED materials in various colors since the development of poly(phenylenevinylene) in 1990 [15]. It has been reported that polyfluorene (PF) [16], poly(phenylenevinylene) (PPV) [17], and poly(methoxy, ethyl-hexyloxy phenylene vinylene) (MEH–PPV) [18] were the representative blue emitting material, green emitting material, and orange and red emitting material, respectively. Furthermore, full color display is enabled by such red, green, blue (R, G, B) color polymers [4,8].

A number of researches have been recently in progress for tuning the colors by introducing a variety of chromophore to PF, the blue emitting material. When chromophore was introduced to PF backbone, aggregation and excimer were suppressed. In addition, the effective energy transfer from PF backbone to chromophore was completed. Then, the high efficiency is acquired and various colors (green, red, white) can be implemented [19,20]. The approaches to introduce chromophore enabling such color tuning include alternating copolymerization between fluorene and chromophore and the random copolymerization implementing micro-dopping (<5 mol%) of low band gap chromophore to blue emitting polymer backbone [21]. For copolymerization by micro-dopping (<5 mol%) of low band gap chromophore to PF backbone, it has been reported that diverse colors including green and yellow can be acquired depending on mol contents and high efficiency is achieved [21,22].

* Corresponding author. Tel.: +82 2 450 3498; fax: +82 2 444 0765.
E-mail address: dkmoon@konkuk.ac.kr (D.K. Moon).

0014-3057/$ - see front matter © 2012 Elsevier Ltd. All rights reserved.
http://dx.doi.org/10.1016/j.eurpolymj.2012.06.002

The representative green chromophore with low band gap is benzothiadiazole(BT) derivatives which are electron deficient. BT derivatives show high PL and EL efficiency because of superior thermal and electrochemical stability. Then, they have been frequently applied to green light emitting polymer [23,24]. Furthermore, porphyrin (POR) derivatives have narrow half-peak width and show red light emission. Thus, they have been used a lot as red dopants in OLED [25–28]. POR derivatives demonstrate high absorption peak around 600 nm caused by strong Q-band absorption and features as light-harvesting antenna component. Accordingly, they can make red emission by effectively absorbing the energy in blue and green emission field [29,30].

This paper selected PF as the host, BT derivatives of 0.02–0.15 mol%, as the green emitter and POR derivatives of 0.05–0.3 mol% as the dopant. Forster energy transfer, charge trapping and charge balance effects between the host and the dopant were investigated. Through the analysis, the optimum content, and effective white and green emitting polymers were acquired.

2. Experimental methods

2.1. Instruments and characterization

Unless otherwise specified, all the reactions were carried out under nitrogen atmosphere. Solvents were dried by standard procedures. All column chromatography was performed with the use of silica gel (230–400 mesh, Merck) as the stationary phase. ^{1}H NMR spectra were performed in a Bruker ARX 400 spectrometer using solutions in $CDCl_3$ and chemical were recorded in ppm units with TMS as the internal standard. Electronic absorption spectra were measured in chloroform using a HP Agilent 8453 UV–Vis spectrophotometer. Photoluminescent spectrum were recorded by Perkin Elmer LS 55 luminescence spectrometer. Cyclic voltammetry experiments were performed with a Zahner IM6eX Potentionstat/Galvanostat. All measurements were carried out at room temperature with a conventional three-electrode configuration consisting of platinum working and auxiliary electrodes and a nonaqueous Ag/AgCl reference electrode at the scan rate of 50 mV/s. The solvent in all experiments was acetonitrile and the supporting electrolyte was 0.1 M tetrabutyl ammonium-tetrafluoroborate. TGA measurements were performed on NETZSCH TG 209 F3 thermogravimetric analyzer. All GPC analyses were made using THF as eluant and polystyrene standard as reference.

2.2. Fabrication and characterization of EL device

The fabricated device structure was ITO/PEDOT:PSS/polymer/BaF_2/Ba/Al. All of the polymer light emitting diodes were prepared using the following device fabrication procedure. The glass/indium tin oxide (ITO) substrates [Sanyo, Japan(10 Ω/γ)] were sequentially lithographically patterned, cleaned with detergent, and ultrasonicated in deionized water, acetone and isopropyl alcohol. Then the substrates were dried on a hotplate at 120 °C for 10 min and treated with oxygen plasma for 10 min in order to improve the contact angle just before the film coating process. Poly(3,4-ethylene-dioxythiophene): poly(styrene–sulfonate) (PEDOT:PSS, Baytron P 4083 Bayer AG) was passed through a 0.45 μm filter before being deposited onto ITO at a thickness of ca. 32 nm through spin-coating at 4000 rpm in air and then dried at 120 °C for 20 min inside a glove box. The light-emitting polymer layer was then deposited onto the film by spin coating a polymer solution in chlorobenzene (1.5 wt.%) at a speed of 1000 rpm for 30 s on top of the PEDOT:PSS layer. The device was thermally annealed at 90 °C for 30 min in a glove box. The device fabrication was completed by depositing thin layers of BaF_2 (1 nm), Ba (2 nm) and Al (200 nm) at pressures less than 10^{-6} torr. The active area of the device was 9.0 mm^2. Finally, the cell was encapsulated using UV-curing glue (Nagase, Japan). EL spectra, Commission Internationale de l'Eclairage (CIE) coordinates, current–voltage, and brightness–voltage characteristics of devices were measured with a Spectrascan PR670 spectrophotometer at the forward direction and a computer-controlled Keithley 2400 under ambient condition.

2.3. Materials

All reagents were purchased from Aldrich, Acros or TCI companies. All chemicals were used without further purification. The following compounds were synthesized following modified literature procedures: 2,2′-(9,9-dioctyl-9H-fluorene-2,7-diyl)bis(4,4,5,5-tetramethyl-1,3, 2-dioxaborolane) **2** [4], 4,7-dibromobenzo[c] [1,2,5] thiadiazole **3** [6] 5,15-bis(hexoxybenzyl)-10,20-bis(4-bromobenzyl)porphyrin [31].

2.3.1. Polymerization

Reaction monomers, $(PPh_3)_4Pd(0)$ (1.5 mol%) and Aliquat 336 were dissolved in a mixture of toluene and an aqueous solution of 2 M K_2CO_3. The solution was refluxed for 72 h with vigorous stirring in nitrogen atmosphere, and then the excess amount of bromobenzene, end capper, was added and stirring continued for 12 h. The whole mixture was poured into methanol. The precipitate was filtered off, purified with methanol, acetone, hexane, chloroform in soxhlet.

PFB02P05: 9,9-Dioctylfluorene-2,7-dibromofluorene **(1)** (0.499 equiv), 2,2′-(9,9-dioctyl-9H-fluorene-2,7-diyl)bis(4,4,5,5-tetramethyl-1,3,2-dioxaborolane) **(2)** (0.50 equiv), 4,7-dibromobenzo[c] [1,2,5] thiadiazole **(3)** (0.0002 equiv), 5,15-bis(hexoxybenzyl)-10,20-bis(4-bromobenzyl)porphyrin **(6)** (0.0005 equiv); yield: 0.19 g (44%); ^{1}H NMR (400 MHz; $CDCl_3$; Me_4Si): δ = 7.85–7.83 (m), 7.71–7.25 (m), 2.11 (m), 1.25–1.13 (m), 0.83–0.79 (m).

PFB02P10: 9,9-Dioctylfluorene-2,7-dibromofluorene **(1)** (0.499 equiv), 2,2′-(9,9-dioctyl-9H-fluorene-2,7-diyl)bis(4,4,5,5-tetramethyl-1,3,2-dioxaborolane) **(2)** (0.50 equiv), 4,7-dibromobenzo[c] [1,2,5] thiadiazole **(3)** (0.0002 equiv), 5,15-bis(hexoxybenzyl)-10,20-bis(4-bromobenzyl)porphyrin **(6)** (0.001 equiv); 0.25 g (58%); ^{1}H NMR (400 MHz; $CDCl_3$; Me_4Si): δ = 7.85–7.83 (m), 7.71–7.25 (m), 2.11 (m), 1.25–1.13 (m), 0.83–0.79 (m).

PFB05P10: 9,9-Dioctylfluorene-2,7-dibromofluorene **(1)** (0.499 equiv), 2,2′-(9,9-dioctyl-9H-fluorene-2,7-diyl)bis (4,4,5,5-tetramethyl-1,3,2-dioxaborolane) **(2)** (0.50 equiv),

4,7-dibromobenzo[c] [1,2,5] thiadiazole **(3)** (0.0005 equiv), 5,15-bis(hexoxybenzyl)-10,20-bis(4-bromobenzyl)porphyrin **(6)** (0.001 equiv); yield: 0.28 g (65%); ^{1}H NMR (400 MHz; $CDCl_3$; Me_4Si): δ = 7.85–7.83 (m), 7.71–7.25 (m), 2.11 (m), 1.25–1.13 (m), 0.83–0.79 (m).

PFB10P10: 9,9-Dioctylfluorene-2,7-dibromofluorene **(1)** (0.499 equiv), 2,2′-(9,9-dioctyl-9H-fluorene-2,7-diyl)bis(4,4,5,5-tetramethyl-1,3,2-dioxaborolane) **(2)** (0.50 equiv), 4,7-dibromobenzo[c] [1,2,5]thiadiazole **(3)** (0.001 equiv), 5,15-bis(hexoxybenzyl)-10,20-bis(4-bromobenzyl)porphyrin **(6)** (0.001 equiv); yield: 0.22 g (51%); ^{1}H NMR (400 MHz; $CDCl_3$; Me_4Si): δ = 7.85–7.83 (m), 7.71–7.25 (m), 2.11 (m), 1.25–1.13 (m), 0.83–0.79 (m).

PFB15P10: 9,9-Dioctylfluorene-2,7-dibromofluorene **(1)** (0.499 equiv), 2,2′-(9,9-dioctyl-9H-fluorene-2,7-diyl)bis(4,4,5,5-tetramethyl-1,3,2-dioxaborolane) **(2)** (0.50 equiv), 4,7-dibromobenzo[c] [1,2,5]thiadiazole **(3)** (0.0015 equiv), 5,15-bis(hexoxybenzyl)-10,20-bis(4-bromobenzyl)porphyrin **(6)** (0.001 equiv); yield: 0.25 g (58%); ^{1}H NMR (400 MHz; $CDCl_3$; Me_4Si): δ = 7.85–7.83 (m), 7.71–7.25 (m), 2.11 (m), 1.25–1.13 (m), 0.83–0.79 (m).

PFB15P20: 9,9-Dioctylfluorene-2,7-dibromofluorene **(1)** (0.499 equiv), 2,2′-(9,9-dioctyl-9H-fluorene-2,7-diyl)bis(4,4,5,5-tetramethyl-1,3,2-dioxaborolane) **(2)** (0.50 equiv), 4,7-dibromobenzo[c] [1,2,5]thiadiazole **(3)** (0.0015 equiv), 5,15-bis(hexoxybenzyl)-10,20-bis(4-bromobenzyl)porphyrin **(6)** (0.002 equiv); yield: 0.3 g (70%); ^{1}H NMR (400 MHz; $CDCl_3$; Me_4Si): δ = 7.85–7.83 (m), 7.71–7.25 (m), 2.11 (m), 1.25–1.13 (m), 0.83–0.79 (m).

PFB15P30: 9,9-Dioctylfluorene-2,7-dibromofluorene **(1)** (0.499 equiv), 2,2′-(9,9-dioctyl-9H-fluorene-2,7-diyl)bis(4,4,5,5-tetramethyl-1,3,2-dioxaborolane) **(2)** (0.50 equiv), 4,7-dibromobenzo[c] [1,2,5]thiadiazole **(3)** (0.0015 equiv), 5,15-bis(hexoxybenzyl)-10,20-bis(4-bromobenzyl)porphyrin **(6)** (0.003 equiv); yield: 0.21 g (49%); ^{1}H NMR (400 MHz; $CDCl_3$; Me_4Si): δ = 7.85–7.83 (m), 7.71–7.25 (m), 2.11 (m), 1.25–1.13 (m), 0.83–0.79 (m).

3. Results and discussion

3.1. Synthesis and characterization

As shown in Scheme 1, total seven polymers were polymerized by Suzuki coupling reaction applying diverse mol ratios, monomer 1, 2, 3 and 6. The yield rate was 41–48%. Polymerization used palladium catalyst(0) and 2 M potassium carbonate solution. Aliquot 336 and toluene were used as surfactant and solution, respectively. Reaction was done at 90 °C for 72 h. End-capping used boromobenzene after the completion of polymerization. All polymers were purified by soxhlet in the order of methanol, acetone, chloroform and chloroform fraction was recovered. All polymers were dissolved in general organic solvents including THF, chloroform, chlorobenzene and dichlorobenze. Film fabricated by spin coating showed transparent film.

Fig. 1 shows ^{1}H NMR spectra. As shown in Fig. 1, the aromatic peak and the proton peak were observed around 7.0–8.0 ppm and around 0.8–5.0 ppm due to aliphatic peak, respectively. As illustrated in Fig. 1, because the proton peak of BT and POR the dopants used in a small quantity (10^{-3}–10^{-4} mol to total monomer), its aromatic and aliphatic peaks were not observed. For dopant ratio below 0.5 mol%, in other PLED research, it was reported that it was difficult to obtain the actual dopnat ratios in polymers using NMR, FT-IR, elemental analysis [32–34]. However as shown in Fig. 1S (see Supplementary data) all polymers showed very minutely increased proton peak in 7.30–7.50 ppm compared to PF, which was estimated to be proton peak of BT, POR derivative. In accordance with the measurement of GPC with polystyrene as the standard as shown in Table 1, the number average molecular weights of all polymers were about 12,500–15,000. Polymerization degree of polymers was similar to that of general EL polymer [26,35]. Polydispersity indicies(PDI) demonstrated a significantly narrow distribution, 1.90–2.58.

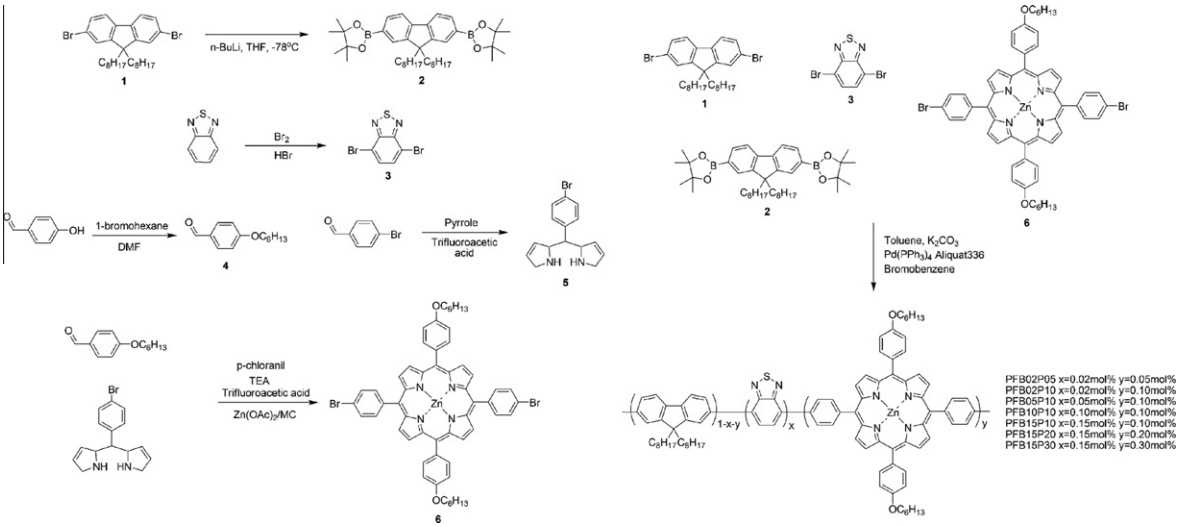

Scheme 1. Scheme of monomer synthesis and polymerization.

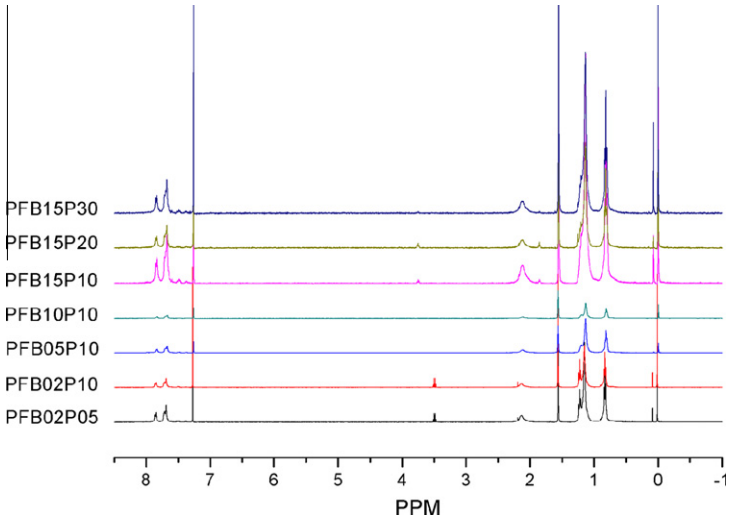

Fig. 1. ^{1}H NMR spectrum of polymers.

Table 1
Physical properties of the polymers.

Polymer	M_n (kg/mol)	M_w (kg/mol)	PDI	T_d[a] (°C)	Φ_{PL}[b]
PFB02P05	15.0	30.5	2.03	422	0.79
PFB02P10	15.0	28.5	1.90	398	0.79
PFB05P10	14.4	37.2	2.58	418	0.74
PFB10P10	12.5	28.8	2.30	408	0.66
PFB15P10	12.6	28.0	2.22	398	0.61
PFB15P20	12.5	26.3	2.10	363	0.55
PFB15P30	13.2	30.4	2.30	408	0.48

[a] Temperature resulting in 5% weight loss based on initial weight.
[b] Solution fluorescence quantum yields measured in chloroform relative to polyfluorene (ca. 1×10^{-5} M, $\Phi_{PL} = 0.79$) in chloroform as a standard.

The thermal properties of the polymers were measured by TGA. 5 wt.% loss point is around 400 °C, which indicated the high thermal stability. The result suggested the applicability to display application field requiring higher thermal stability than 300 °C [31]. All polymers exhibit similar thermal properties as PF. This means that introducing such small amount of emitter unit into polyfluorene backbone does not affect the rigidity of the resulting copolymers. When the temperature was higher than 400 °C, the thermal properties were quite different. As shown in Fig. 2S (see Supplementary data), there was an evident weight loss from 400 to 500 °C, up to 45–50%. This prominent weight loss can be inferred from the degradation of the skeletal PF backbone chain structure. In this stage, the PF backbone may be decomposed to oligomers or other short chain structures [36].

3.2. Optical and electrochemical properties

Fig. 2 showed UV–vis spectra after all polymers were dissolved in chloroform and formed as solution and film. As shown in Fig. 2, the maximum absorption peak (λ_{max}) for solution state was observed between 386 and 389 nm which was similar to the absorption peak (λ_{max} = 384 nm) of PF [33,34]. For film state, the maximum absorption peak of all polymers was λ_{max} = 382 nm, 4–7 nm blue-shifted than the solution state. The result was caused by π–π^* transition distribution between polymer chains occurred while fluorene polymer forms the film [37]. The absorption peaks of BT and POR derivatives, the dopants, were not observed because the quantity of dopants was low concentration.

Fig. 3 show the photoluminescent spectra of all polymers in solution and film state. As shown in Fig. 3 (a), the maximum emission peak of PL spectra in the solution state was observed around 418 nm (λ_{max} = 418 nm), and the shoulder peak appeared around 440 nm. It is similar to the emission peak (λ_{max} = 420, 442 nm) of polyfluorene solution. Moreover, the emission peak of a dopant was not found because the quantity of a dopant was its low concentration and the intermolecular interaction occurs in the solution state [19].

For PL spectra of film shown in Fig. 3 (b), the more BT content increased, the more the 520 nm emission peak increased unlike the solution state (Fig. 3(b) (2–5)). 612 nm emission peak caused by POR peak increased in accordance with the increase of BT and POR. For polymers whose BT contents were more than 0.05 mol% (Fig. 3(b) (3–7)), PL spectrum around 520 nm increased in accordance with the increase of BT contents because of the forster energy transfer from fluorene derivatives to BT derivatives [38]. However, for the polymers which were synthesized with POR contents increased and BT contents kept at constant level of 0.1 mol% (Fig. 3(b) (5), (6)), the emission peak around 520 nm demonstrated the increasing tendency. Furthermore, when POR contents were more than 0.3 mol%, 520 nm peak reduced and the peak around 612 nm increased (Fig. 3(b) (6), (7)). Accordingly, increase of the contents of POR derivatives effectively activated Forster energy transfer from fluorene to POR rather than that from fluorene to BT derivatives [16,39,40].

Fig. 3S (see Supplementary data) illustrates UV–vis spectrum of POR monomer and PL spectrum of polyfluorene. Fig. S1 confirmed that absorption spectrum area of POR

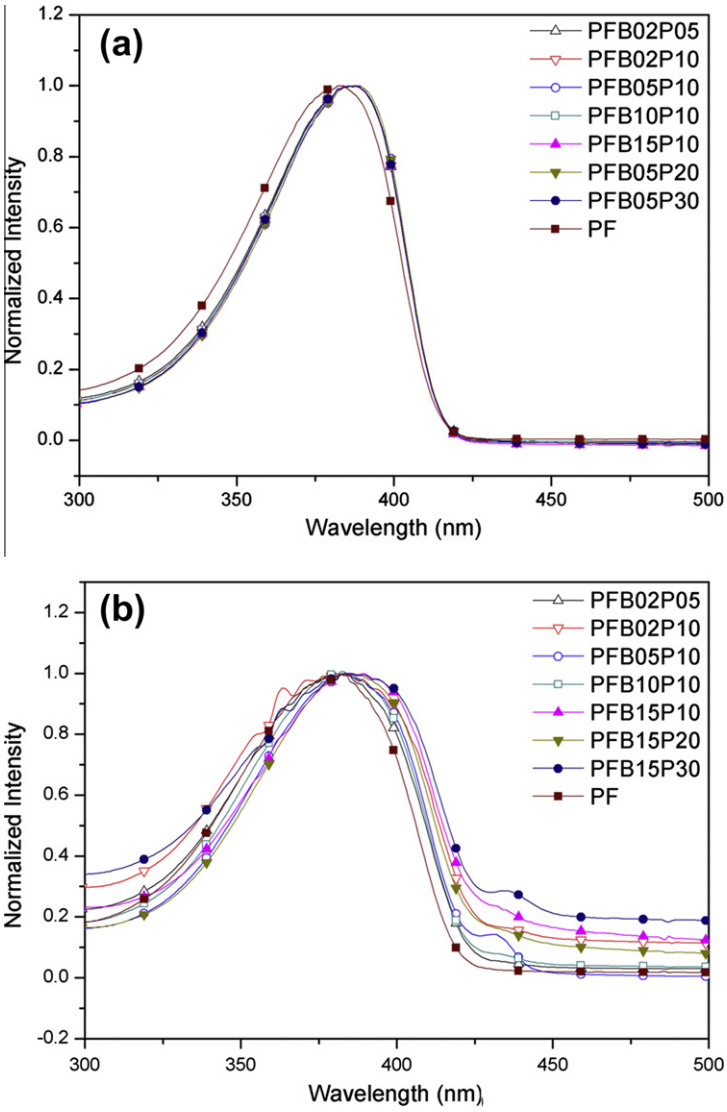

Fig. 2. UV–Vis absorption spectra (a) in solution (b) in thin film of polymers.

derivatives was overlapped to PL spectrum of PF. It means that POR derivative effectively absorbed PF emission energy. On the contrary, in accordance with Shu and co-workers, it was reported that for BT area, the relatively small area was overlapped [39]. Accordingly, the copolymer in this paper will have more effective Forster energy transfer from fluorene derivatives to POR derivatives than to BT derivatives. Such results were confirmed in PFB15P20 (Fig. 3(b) (6)), PFB15P30 (Fig. 3(b) (7)) PL spectra as shown in Fig. 3(b). PL spectrum of PFB15P30 polymer in Fig. 3(b) illustrated that the emission peak around 520 nm caused by BT went down as compared to PFB15P20 polymer and the emission peak around 612 nm went up caused by POR. On the basis of such results, the copolymers in this paper proved the more effective Forster energy transfer from fluorene derivatives to POR derivatives than to BT derivatives.

Fig. 4 described the HOMO and LUMO levels acquired using the onset values of Cyclicvoltammetry. The scan rate of Cyclicvolammetry was set at 50 mV/s and the reference electrode was Ag/AgCl. The HOMO value was calculated by the formula below after compensation using Ferrocene.

$$\mathrm{HOMO(eV)} = -4.8 - (\mathrm{E_{onset}} - \mathrm{E_{1/2}(Ferrocene)})$$

The lowest unoccupied molecular orbital (LUMO) levels were acquired from the difference between HOMO level of polymers and optical band gap, the UV–Vis absorption onset value of polymer film. Table 2 illustrates the HOMO and LUMO levels of polymers and optical band gap measured. HOMO level of polymers −5.68 to −5.72 eV, and LUMO level −2.68 to −2.77 eV. Increasing contents of BT and POR dopants caused slight increase of HOMO level because HOMO levels of BT and POR, the dopants, were higher than HOMO level of PF(−5.77 eV) and higher contents of

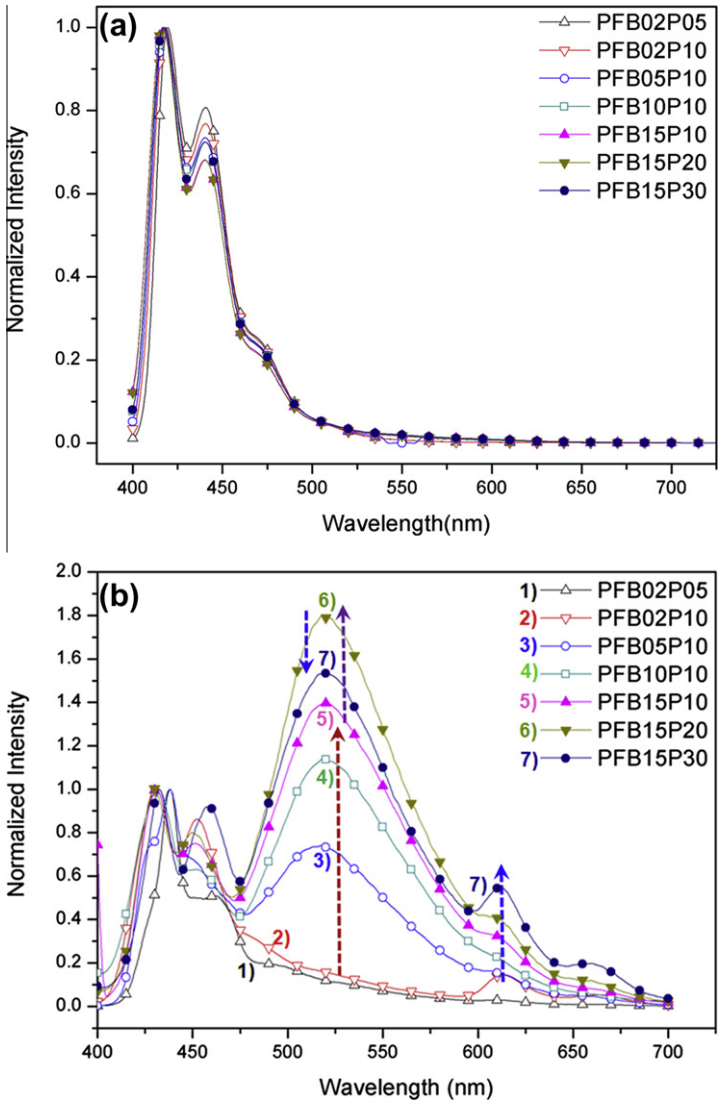

Fig. 3. PL emission spectra (a) in solution (b) in thin film of polymers.

dopants had impact on energy level through interaction with polymer backbone [19]. Fig. 4 shows the energy band diagram of PF, POR and BT derivatives. The energy levels of PF, the host, and POR, the dopant, were measured through CV and UV–Vis spectroscopy. The energy level of BT referred to the reference [7,8]. Fig. 4 indicated that the energy levels of BT and POR, the dopants, existed between HOMO and LUMO level of PF. On the basis of the results, it is estimated that energy transfer is activated by BT and POR, the dopants, in PF and will induce the effective charge trapping [26,40]. Table 2 summarizes the optical and electrochemical properties.

3.3. Electroluminescence properties and current–voltage–luminance characteristics

Fig. 5 demonstrated electroluminescent spectra of EL device. Fig. 6 (a and b) showed the brightness–voltage and efficiency–current density features of EL device, respectively. The data of Fig. 6 (a and b) is summarized in Table 3. The device was made in the ITO/PEDOT:PSS/polymer/BaF_2/Ba/Al structure as shown in Fig. 6 (a) inset and the emission layer was made to be 70–80 nm thick by spin-coating. As shown in Fig. 5, for PFB02P05, PFB02P10 (Fig. 5 (1,2)) polymers, the energy transfer from fluorene derivatives to dopants was partially made so that overall EL spectrum became broad. On the contrary, for PFB05P10–PFB15P30 (Fig. 5 (3–7)) polymers whose BT derivatives contents were more than 0.05 mol%, most energy transfer occurred from fluorene derivatives to BT derivatives. Accordingly, the spectrum of 400–450 nm was significantly reduced and the spectrum of 500–550 nm was remarkably expanded. Furthermore, as shown in the spectra of PFB15P10, PFB15P20, and PFB15P30 polymers (Fig. 5 (5–7)), the more the contents of POR derivatives increased, the more the intensity of 600–700 nm spectrum went up. It was the similar results to PL spectra.

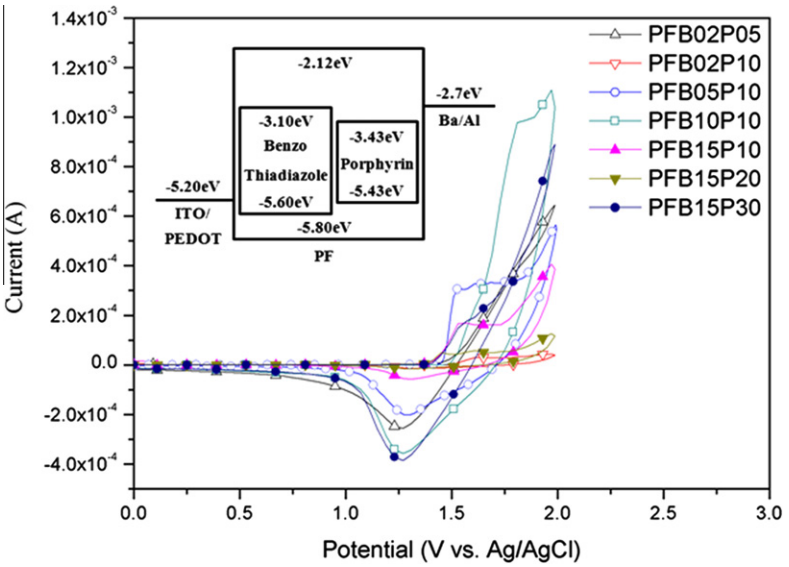

Fig. 4. Cyclic voltammograms of polymers and band diagram of PF, BT and POR.

Table 2
Optical and electrochemical properties of polymers.

Polymer	Solution, λ_{max}(nm)		Film, λ_{max}(nm)		E_{HOMO}(eV)	E_{LUMO}(eV)
	Absorption	Emission	Absorption	Emission		
PF	384	420, 442	382	430, 444	5.77	2.77
PFB02P05	386	420, 441	382	438, 462	5.77	2.77
PFB02P10	387	418, 441	382	431, 452	5.77	2.77
PFB05P10	389	418, 441	382	438, 518	5.74	2.74
PFB10P10	386	418, 440	382	432, 452, 519	5.77	2.77
PFB15P10	387	417, 440	382	431, 451, 520	5.72	2.72
PFB15P20	388	417, 440	382	430, 450, 522	5.68	2.68
PFB15P30	388	417, 440	382	432, 458, 521	5.68	2.68

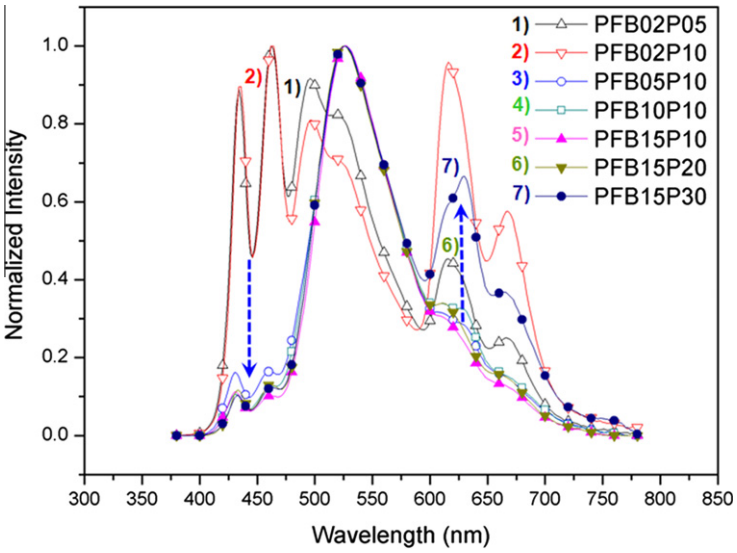

Fig. 5. EL luminescence spectra of polymers.

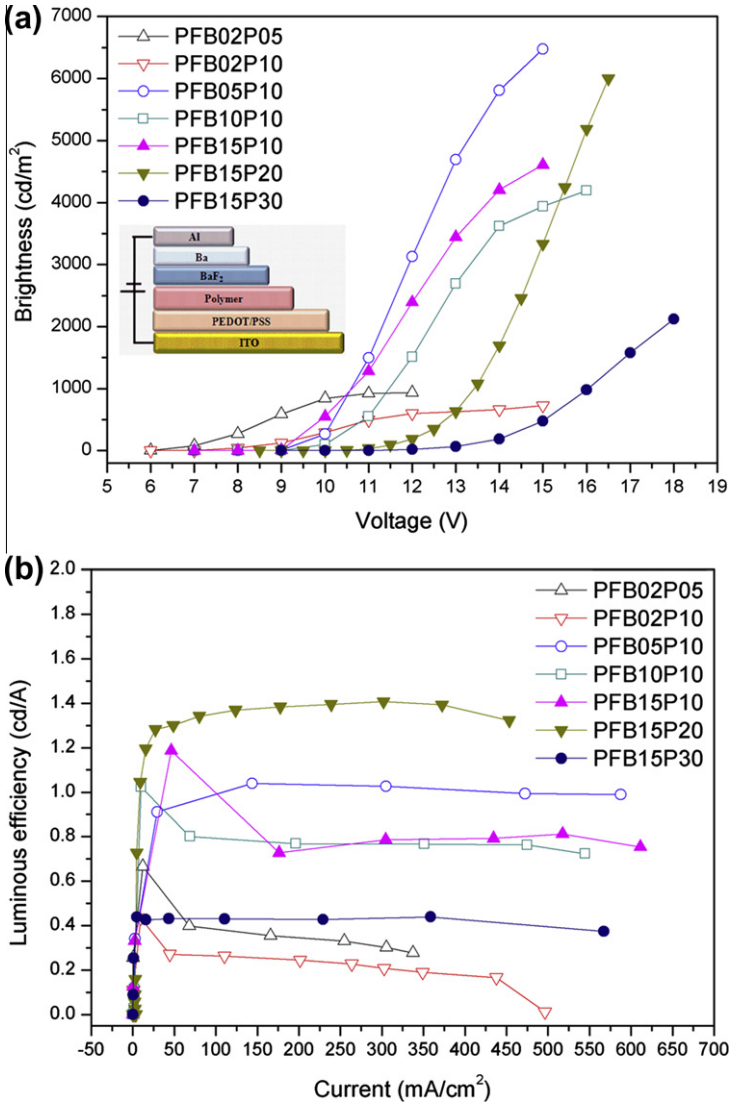

Fig. 6. (a) Voltage–luminance (*V–L*), (b) current density–luminous efficiency (*J–LE*) curve.

Table 3
Summary of EL Device Performances of polymers.

polymer	EL emission λ_{max}(nm)	Luminous efficiency (cd/A)	Power Efficiency (lm/W)	Maximum brightness (cd/m^2)	CIE coordinate (x, y)
PFB02P05	430, 462, 496, 616, 666	0.66	0.29	936	(0.29, 0.34)
PFB02P10	436, 464, 496, 616, 668	0.43	0.17	726	(0.36, 0.34)
PFB05P10	430, 460, 526, 630, 666	1.04	0.29	6474	(0.31, 0.49)
PFB10P10	432, 462, 526, 360, 666	1.02	0.32	4194	(0.33, 0.53)
PFB15P10	432, 460, 526, 630, 666	1.18	0.37	4608	(0.31, 0.51)
PFB15P20	434, 462, 526, 630, 666	1.40	0.32	5997	(0.33, 0.54)
PFB15P30	434, 462, 526, 630, 666	0.43	0.11	2121	(0.38, 0.50)

The difference between PL spectra and EL spectra was identified in general. The green and red emission (λ_{max} = 562, 630 nm) was relatively higher than blue emission (λ_{max} = 432 nm) in EL spectra differently from PL spectra. On the basis of the results above, it was confirmed that lower energy levels of BT and POR derivatives worked toward charge trapping site. The results are same as the HOMO and LUMO levels of dopants identified by electrochemical measurement [19,26,35]. As shown in Table 3, CIE coordinates of PFB02P05, and PFB02P10 (Fig. 5 (1,2))

polymers were (0.29, 0.34), and (0.36, 0.34), respectively, and their white emissions were closer to pure white (0.33, 0.33).

For voltage–luminecence(*V–L curve*) in Fig. 6 (a), increasing contents of BT and POR dopants induced increasing tendency of 'turn on voltage' from 6 to 9 V because BT and POR derivatives activate charge-trapping phenomena [19]. The best EL performance was observed in PFB15P20 polymer. The green emission was identified with the maximum efficiency of 1.40 cd/A, the maximum brightness of 5997 cd/m^2, and CIE coordinates of (0.33, 0.54). As shown in Fig. 6 (b), PFB15P20 showed the stable luminous efficiency which was not reduced along with the increase of current density. PFB15P20 polymer had stable and the best performance because the ratio of PFB15P20 polymer dopants was well balanced between electron and hole injection in the device and energy transfer was effectively processed between fluorene derivatives, and BT and POR derivatives [35]. PFB15P30 polymer had lower EL performance than PFB15P10 and PFB15P20 polymers because increasing contents of porphyrin derivatives worked toward charge trapping site along polymer backbone and exciton quenching occurred [19].

Fig. 4S (see Supplementary data) demonstrated CIE coordinate (1931) of polymers. For PFB02P05 and PFB02P10 polymers, it was observed in the white emission area, but in green emission with the increasing contents of dopants. Furthermore, for PFB15P30 polymers whose POR contents were 0.3 mol%, the color coordinates made red-shift toward the *X*-axis and yellowish-green emission appeared because of strong red emission caused by more energy transfer from fluorene derivatives to POR derivatives than to BT derivatives as shown in PL spectra. In consequence, it was confirmed that color tune was observed in the order of white, green and yellowish–green depending on the contents of dopants.

4. Conclusion

We successfully synthesized color tunable polymers containing BT, POR to a fluorene backbone, blue chromophore. The synthesized PFBP series polymers displayed good solubility and thermal stability. In PL spectra, increase of the contents of POR derivatives showed effective Forster energy transfer from fluorene to POR rather than that from fluorene to BT derivatives. In EL device, PFB15P20 polymer had stable and the best performance because the ratio of PFB15P20 polymer dopants was well balanced between electron and hole injection in the device and energy transfer was effectively processed between fluorene derivatives, BT and POR derivatives. Its luminous efficiency, maximum brightness, CIE coordinate were 1.40 cd/A, 5997 cd/m^2, (0.33, 0.54) close to green, respectively. CIE coordinates of PFB02P05, PFB02P10 polymers showed broad spectra and CIE coordinates of PFB02P05, PFB02P10 polymers showed (0.29, 0.34), (0.36, 0.34), respectively, and their emissions were closer to pure white (0.33, 0.33).

Appendix A. Supplementary data

Supplementary data associated with this article can be found, in the online version, at http://dx.doi.org/10.1016/j.eurpolymj.2012.06.002.

References

[1] Friend RH, Gymer RW, Holmes AB, Burroughes JH, Marks RNC, Taliani C, et al. Electroluminescence in conjugated polymers. Nature 1999;397(6715):121–8.

[2] Lu W, Kuwabara J, Kanbara T. Polycondensation of dibromofluorene analogues with tetrafluorobenzene via direct arylation. Macromolecules 2011;44(6):1252–5.

[3] Song HJ, Lee JY, Song IS, Moon DK, Haw JR. Synthesis and electroluminescence properties of fluorene·anthracene based copolymers for blue and white emitting diodes. J Ind Eng Chem 2011;17(2):352–7.

[4] Lee JY, Song IS, Moon DK, Haw JR. Synthesis of fluorene- and anthracene-based π-conjugated polymers and dependence of emission range and luminous efficiency on molecular weight. J Ind Eng Chem 2010;16(3):395–400.

[5] Lee JY, Shin WS, Haw JR, Moon DK. Low band-gap polymers based on quinoxaline derivatives and fused thiophene as donor materials for high efficiency bulk-heterojunction photovoltaic cells. J Mater Chem 2009;19(28):4938–45.

[6] Lee JY, Kim SH, Song IS, Moon DK. Efficient donor–acceptor type polymer semiconductors with well-balanced energy levels and enhanced open circuit voltage properties for use in organic photovoltaics. J Mater Chem 2011;21(41):16480–7.

[7] Krebs FC. Polymer solar cell modules prepared using roll-to-roll methods: Knife-over-edge coating, slot-die coating and screen printing. Sol Energy Mater Sol Cells 2009;93(4):465–75.

[8] Gustafsson CG, Treacy Y, Klavetter GM, Colaneri F, Heeger AJ. Flexible light-emitting diodes made from soluble conducting polymers. Nature 1992;357(6378):477–9.

[9] Lee JY, Song KW, Ku JR, Sung TH, Moon DK. Development of DA-type polymers with phthalimide derivatives as electron withdrawing units and a promising strategy for the enhancement of photovoltaic properties. Sol Energy Mater Sol Cells 2011;95(12):3377–84.

[10] Lee BL, Yamamoto T. Syntheses of new alternating CT-type copolymers of thiophene and pyrido[3,4-b]pyrazine units: their optical and electrochemical properties in comparison with similar CT copolymers of thiophene with pyridine and quinoxaline. Macromolecules 1999;32(5):1375–85.

[11] Mcculloch I, Heeney M, Bailey C, Genevicius K, Macdonald I, Shkunov M, et al. Liquid-crystalline semiconducting polymers with high charge-carrier mobility. Nature materials 2006;5(4):328–33.

[12] Yasuda T, Imase T, Yamamoto T. Synthesis, characterization, and optical and electrochemical properties of new 2,1,3-benzoselenadiazole-based CT-type copolymers. Macromolecules 2005;38(17):7378–85.

[13] Tanimoto A, Yamamoto T. Synthesis of *n*-type poly(benzotriazole)s having p-conducting and polymerizable carbazole pendants. Macromolecules 2006;39(10):3546–52.

[14] Alam MM, Jenekhe SA. Polybenzobisazoles are efficient electron transport materials for improving the performance and stability of polymer light-emitting diodes. Chem Mater 2002;14(11):4775–80.

[15] Burroughes JH, Bradley DDC, Brown AR, Marks RN, Mackay K, Friend RH, et al. Light-emitting diodes based on conjugated polymers. Nature 1990;347(6293):539–41.

[16] Pei Q, Yang Y. Efficient photoluminescence and electroluminescence from a soluble polyfluorene. J Am Chem Soc 1996;118(31):7416–7.

[17] Tan Z, Tang R, Zhou E, He Y, Yang C, Xi F, et al. Electroluminescence and photovoltaic properties of poly(p-phenylene vinylene) derivatives with dendritic Pendants. Appl Polym Sci 2008;107(1):514–21.

[18] Deng XY, Lau WM, Wong KY, Low KH, Chow HF. High efficiency low operating voltage polymer light-emitting diodes with aluminum cathode. Appl Phys Lett 2004;84(18):3522–4.

[19] Park MJ, Lee JH, Jung IH, Park JH, Hwang DH, Shim HK. Synthesis, characterization, and electroluminescence of polyfluorene copolymers with phenothiazine derivative their applications to high-efficiency red and white PLEDs. Macromolecules 2008;41(24):9643–9.

[20] Hou Q, Xu Y, Yang W, Yuan M, Peng J, Cao YJ. Novel red-emitting fluorene-based copolymers. J Mater Chem 2002;12(10):2887–92.

[21] Cho NS, Hwang DH, Lee JI, Jung BJ, Shim HK. Synthesis and color tuning of new fluorene-based copolymers. Macromolecules 2002;35(4):1224–8.
[22] Klärner G, Lee JI, Davey MH, Miller RD. Exciton migration and trapping in copolymers based on dialkylfluorenes. Adv Mater 1999;11(2):115–9.
[23] Fung MK, Lai SL, Tong SW, Bao SN, Lee CS. Distinct interfaces of poly (9,9-dioctylfluorene-co-benzothiadiazole) with cesium and calcium as observed by photoemission spectroscopy. J Appl Phys 2003;94(9):5763–70.
[24] Liu J, Bu L, Dong J, Zhou Q, Geng Y, Ma D, et al. Green light-emitting polyfluorenes with improved color purity incorporated with 4,7-diphenyl-2,1,3-benzothiadiazole moieties. J Mater Chem 2007;17(28):2838.
[25] Li B, Xu X, Sun M, Fu Y, Yu G, Liu Y, et al. Porphyrin-cored star polymers as efficient nondoped red light-emitting materials. Macromolecules 2006;39(1):456–61.
[26] Li H, Xiang N, Wang L, Zhao B, Shen P, Lu J, et al. Synthesis and white electroluminescent properties of multicomponent copolymers containing polyfluorene, oligo(phenylenevinylene), and porphyrin derivatives. J Polym Sci Part A: Polym Chem. 2009;47(20):5291–303.
[27] Zhua LJ, Wanga J, Renga TG, Lia CY, Guoa DC, Guo CC. Effect of substituent groups of porphyrins on the electroluminescent properties of porphyrin-doped OLED devices. J. Phys Org Chem 2010;23(3):190–4.
[28] Li B, Li J, Fu Y, Bo Z. Porphyrins with four monodisperse oligofluorene arms as efficient red light-emitting materials. J Am Chem Soc 2004;126(11):3430–1.
[29] Hasobe T, Sandanayaka ASD, Wadac T, Arakic Y. Fullerene-encapsulated porphyrin hexagonal nanorods. An anisotropic donor–acceptor composite for efficient photoinduced electron transfer and light energy conversion. Chem Commun 2008:3372–4.
[30] Xiang N, Liu Y, Zhou W, Huang H, Guo X, Tan Z, et al. Synthesis and characterization of porphyrin-terthiophene and oligothiophene p-conjugated copolymers for polymer solar cells. Euro Polym J 2010;46(5):1084–92.
[31] Lee JY, Song HJ, Lee SM, Lee JH, Moon DK. Synthesis and investigation of photovoltaic properties for polymer semiconductors based on porphyrin compounds as light-harvesting units. Euro Polym J 2011;47(8):1686–93.
[32] Liu J, Gao B, Cheng Y, Xie Z, Geng Y, Wang L, et al. Novel white electroluminescent single polymer derived from fluorene and quinacridone. Macromolecules 2008;41(4):1162–7.
[33] Hsieh BY, Chen Y. Copolyfluorenes containing phenothiazine or thiophene derivatives: synthesis, characterization, and application in white-light-emitting diodes. J Polym Sci Part A: Polym Chem 2009;47:833–44.
[34] Lee SK, Jung BJ, Ahn T, Jung YK, Lee JI, Kang IN, et al. White electroluminescence from a single polyfluorene containing bis-DCM units. J Polym Sci Part A: Polym Chem 2007;45(15):3380–90.
[35] Park MJ, Lee JH, Park JH, Lee SK, Lee JI, Chu HY, et al. Synthesis and electroluminescence of new polyfluorene copolymers with phenothiazine derivative. their application in white-light-emitting diodes. Macromolecules 2008;41(9):3063–70.
[36] Xu J, Zhang Y, Hou J, Wei Z, Pu S, Zhao J, et al. Low potential electrosyntheses of free-standing polyfluorene films in boron trifluoride diethyl etherate. Euro Polym J 2006;42(5):1154–663.
[37] Neher D. Polyfluorene homopolymers: conjugated liquid-crystalline polymers for bright blue emission and polarized electroluminescence. Macromol Rapid Commun 2001;22(17):1365–85.
[38] Luo J, Li X, Hou Q, Peng J, Yang W, Cao Y. High-efficiency white-light emission from a single copolymer: fluorescent blue, green, and red chromophores on a conjugated polymer backbone. Adv Mater 2007;19(8):1113–7.
[39] Chuang CY, Shih PI, Chien CH, Wu FI, Shu CF. Bright-white light-emitting devices based on a single polymer exhibiting simultaneous blue, green, and red emissions. Macromolecules 2007;40(2): 247–52.
[40] Chen Q, Liu N, Ying L, Yang W, Wu H, Xu W, et al. Novel white-light-emitting polyfluorenes with benzothiadiazole and Ir complex on the backbone. Polymer 2009;50(6):1430–7.